

Article citation info:

Karpenko M, Prentkovskis O, Šukevičius Š. Research on high-pressure hose with repairing fitting and influence on energy parameter of the hydraulic drive. *Eksploracja i Niezawodność – Maintenance and Reliability* 2022; 24 (1): 25–32, <http://doi.org/10.17531/ein.2022.1.4>.

Research on high-pressure hose with repairing fitting and influence on energy parameter of the hydraulic drive

Indexed by:



Mykola Karpenko^a, Olegas Prentkovskis^a, Šarūnas Šukevičius^a

^aVilnius Gediminas Technical University, Department of Mobile Machinery and Railway Transport, Plytinės st. 27, LT-10105, Vilnius, Lithuania

Highlights

- High-pressure hoses and junctions failure influence to flow parameters were analyzed.
- Comparative analysis between non-repaired and repaired high-pressure hoses were performed.
- Numerical simulations (CFD) and experimental measurement applied in the research.
- Pressure drops and flow coefficients at non-repaired and after maintenance hose was obtained.
- Research find the insignificant power losses in repaired hose compared to standard hose.

Abstract

Reliability and maintenance analysis of transport machines hydraulic drives, basically focused to power units: pumps, cylinders etc., without taking in to account junction elements. Therefore, this paper proposes a research analysis on high-pressure hoses and junctions during technical maintenance. Comparative analysis of fluid behavior and energy efficiency inside non-repaired and repaired high-pressure hoses is presented in this research. Theoretical and experimental research results for hydraulic processes inside high-pressure hose is based on the numerical simulations using Navier–Stokes equations and experimental measurement of fluid flow pressure inside high-pressure hoses. Research of fluid flow dynamics in the hydraulic system was made with main assumptions: system flow rate in the range from 5 to 100 l/min, diameter of the hoses and repairing fitting are 3/8". The pressure drops, power losses, flow coefficients at non-repaired and after maintenance hose was obtained as a result. Simulation results were verified by running physical experiments to measure the pressure losses.

Keywords

This is an open access article under the CC BY license (<https://creativecommons.org/licenses/by/4.0/>)

high-pressure hose, fitting, maintenance, energy, pipeline, fluid flow, numerical modeling, hydraulic system, CFD.

1. Introduction

Due to the wide use of hydraulic drives in machines and mechanisms in various technical area from the transport engineering [3, 16, 17] to aviation engineering [32] and even in industrial sectors [6, 25], there is an objective need for monitoring the technical condition of its elements. Modern hydraulic drive of any mobile machine or industrial system are complex, branch and usually considering from a lot different hydraulic elements (pumps, valves, throttles, cylinders and etc.). For connection all hydraulic elements to one system - using a special object which is high-pressure hose. High-pressure hoses is metal or flexible composite pipelines [5, 26, 43] designed to transmit hydraulic forces and working fluid between units of hydraulic drive. The wall of high-pressure hoses is multilayer, consisting of rubber and reinforcing layers. The number of reinforcing layers depends on the required characteristics of high-pressure hose and can vary from one to seven layers. However, according to [22, 34], the most common in the hydraulic drive of a transport-technological machine is the high-pressure hoses with one and two metal reinforcing layers (Fig.1a).

The composite pipelines and high-pressure hoses is being used as the main components for hydraulic systems, especially in strong vi-

bration environments. These exploitation conditions may cause composite pipe fatigue or even long-term damage [30]. In the research [31] pointed that from a total of 106 flexible pipe failure or damage incidents 20% of flexible pipes were found to have experienced some form of damage or failure. 2/3 cases occurred during long-term using and 1/3 cases during normal period of operation, from this 20% amount. 32 failures requires replace flexible pipes, rest amount can be repaired, from these total 106 cases. Hose defects and malfunctions were extensively studied and discussed by specialists and researchers. According to [10 and 21], there are two main types of to the high pressure hoses damage, that produce failure:

- A) External damage. Caused by environmental influences and loads or friction of a high pressure hose against a surface shown at Fig 1b.
- B) Internal damage (damage to the inner layers, shown at Fig. 1c). Caused by high pressures by fluid pulsation inside the hose, by non-compliance with frequency characteristics or other factors (e.g. aggressive oil, flexural vibrations of hose, etc.).

External damage of high-pressure hoses is easily diagnosed by visual inspection, but internal damage diagnosed without special tests

E-mail addresses: M. Karpenko (ORCID: 0000-0002-1915-5219): mykola.karpenko@vilniustech.lt, O. Prentkovskis (ORCID: 0000-0003-0910-591X): olegas.prentkovskis@vilniustech.lt, Š. Šukevičius (ORCID: 0000-0002-1393-1731): sarunas.sukevicius@vilniustech.lt

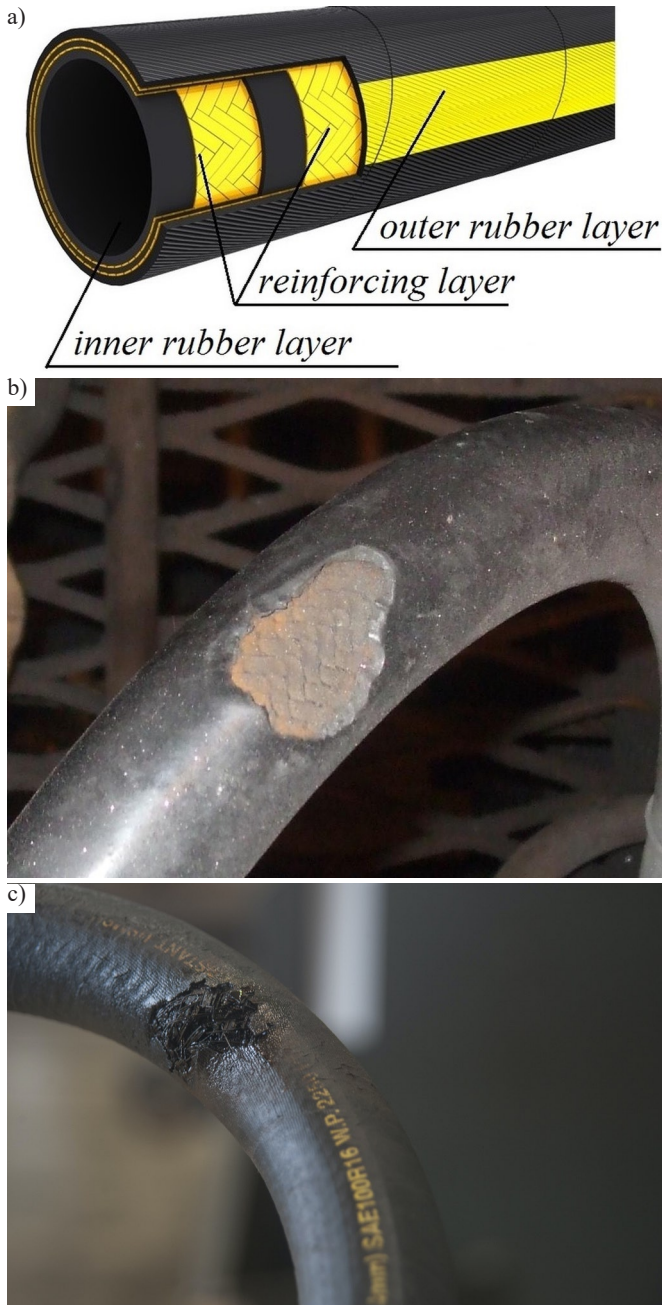


Fig. 1. Views of high pressure hose: a) high-pressure hose with two metal braids; b) external damage of high-pressure hose; c) result from internal damages of high-pressure hose

is impossible, until the hoses are not braked. Failure of hydraulic hoses is a critical problem, factors associated with hoses failure are material characteristics [38], hose geometry [11], environmental conditions [10], internal or external loadings [27], and manufacturing flaws [8]. The interaction of these factors is very complex to analyses. The high-pressure hose with external and internal damages could be operated for some time, but dynamic flow parameters and reliability of hydraulic system will be reduced. Damage to the external or internal layer of the high-pressure hose will not only effect on the energy and reliable parameters of the hydraulic system, but can lead to accidentally lead to the break of the high-pressure hose during exploitation. The volumetric surface defects of high-pressure hose appear because of corrosion or erosion-corrosion processes in the reinforcing layer and these areas considerably decreasing the high-

pressure hose strength. [28]. It is important to find out the cause of the external defects and understand the destruction process in order to reduce the risk of injury, equipment failure, energy losses or environmental disaster. The sooner the fact of damage is established and the high-pressure hose is technically serviced or replaced, the lower the risk of failure of the entire hydraulic drive and energy losses, the more reliable the system [29].

Therefore, it is very important, to study fretting fatigue and failure mechanism of hoses and fittings after maintenance to improve the reliability of hydraulic hoses system in a future [44]. The evaluation of maintenance costs of pipelines system should not only take in to account the present repair cost hydraulic system, but also the value of future maintenance cost using this repaired system, according to the [37]. That is why, after repair high-pressure hose and installation back to the hydraulic drive system there is a need to study the influence of the repair performance to the fluid dynamic inside the hose, as well as to the reliability and energy parameters.

2. Repair of damaged high-pressure hose

Repair of damaged high-pressure hoses or it's segments is a complicated operation which require to remove hose from the hydraulic drive. Therefore repair actions are performed only in case of defect that and in special zones during machine maintenance [5]. Usually, if high-pressure hose is relatively short, it is replaced with the new one. In case if high-pressure hose is longer than one meter and have an external damages, it can be repaired and installed back (economically better solution) [13]. One way decrease maintenance cost is to apply repairing fitting (hose junction) in the area of high-pressure hose defect instead of replacing hose with the new hose. This technique involves that the damaged segments can be cutted off and hose repaired with a hose junction, scheme of high-pressure hose repairing with a repair fitting is showed in Fig. 2. The main idea of the reinforcement techniques is to transfer hoop stress [33], caused by the internal fluid pressure, from the defected area and cutted ends of the high-pressure hose to the steel sleeves and repair fitting.

The repaired hose should withstand not only internal fluid pressure but also external interference, such as environment loads, friction and heat transfer. This is because wide part of high-pressure hose external damage are the result of damage due hose friction with other surfaces or environment influences [39]. As a result, the fluid behaviour and it influence on energy consumption inside the repaired hose with repair fitting is required determination and compared with the fluid behaviour in the non-repair hose, since, the sudden cross-section changes hoses influence on pressure and energy parameters of the hydraulic system [19]. Unfortunately, during reviewing of similar researches on high-pressure hoses the mention problematic doesn't was found. The current research is proposes a model for investigation fluid behaviour

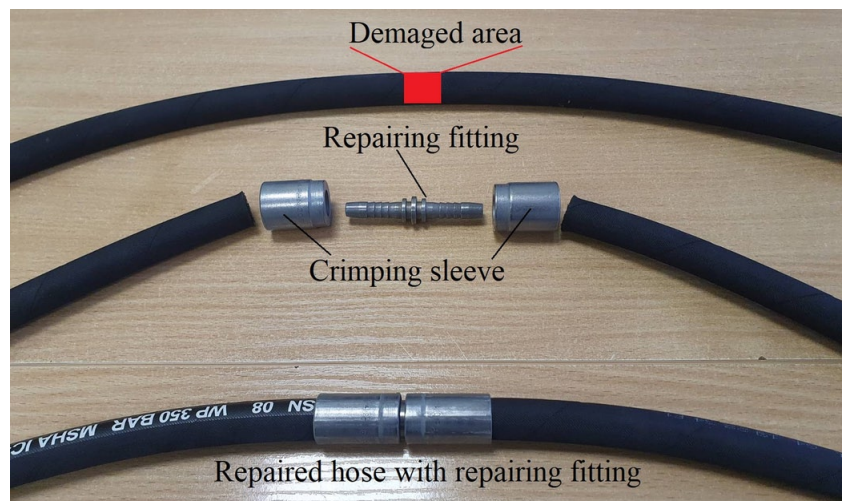


Fig. 2 Scheme of high-pressure hose repairing with a repairing fitting (hose junction)

inside repaired high-pressure hoses and it influences on energy parameter of hydraulic drive after maintenances.

3. Research objects

In presented research, for comparing analysis between flow characteristics inside repaired and non-repaired high-pressure hoses was used two metal braid reinforced hydraulic hose (2SN) according to European Standard [9] and repairing fitting connector (hose junction)

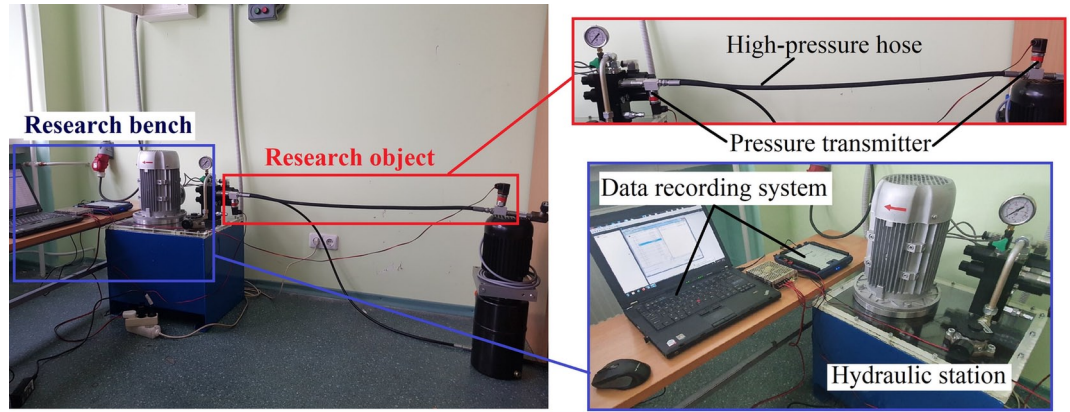


Fig. 4. An experimental bench for measuring of pressure drop inside a high-pressure hoses

Table 1. Physical and geometrical parameters of the research objects

Research object	Inner diameter	Outer diameter	Max working pressure	Weight
High-pressure hose	3/8" or 9.5 mm	19 mm	350 bar	0.63 kg/m
Repair fitting	6.5 mm	3/8" or 9.5 mm	not indicated	0.04 kg

according to International Standard [15]. The high-pressure hose with conditional passage 06 DASH (which is equal to the diameters 3/8" or 9.5 mm) and the same size hose junction for repairing is accepted for research. Parameters of used high-pressure hoses and hose junction in the research is presented in Table 1.

For numerical simulation, the cross-section of the 3D model of high-pressure hose with repair fitting is created. The cut in the connection of repair fitting (hose junction) and high-pressure hose is shown in Fig. 3.

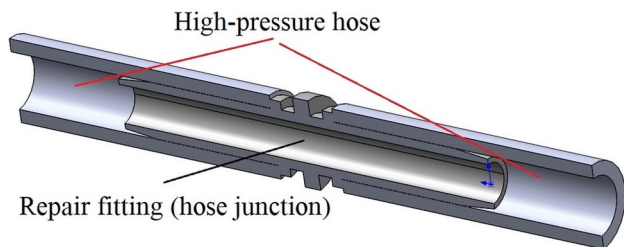


Fig. 3. View of cut in the connection of the repair fitting and high-pressure hose

The main issue in high-pressure hose with repair fitting connection is changes in the size and configuration of the cross-section area of the flow stream inside hydraulic line. The length of high-pressure hoses, used in the current research is 1 meter. Presented high-pressure hose and hose junction are International Certificate and are used in the most mobile machinery, vehicle and aviation hydraulic drives.

4. Pre-experimental part of the research

Pre-experimental part was conducted towards establishing the evidence of proposed research direction. The pre-experimental part of the current research included the measurement and analysis of pressure drop inside a high-pressure hose and high-pressure hose with repair fitting. The obtained results from the pre-experimental measurements is used for boundary conditions of numerical simulation model.

The experimental bench for the pre-experimental research is shown in Fig. 4. The main parameters in the research bench: fluid pressure ~ 2.5 MPa; flow rate ~ 50 l/min; high-pressure hose is 3/8" (9.5 mm); length of hoses is 1 meter; hose fittings connection standard and repairing fitting size – 06 DASH. The pre-experimental test performed via Multiple Measurement Design and based on One-Sample Statistical Method with Estimating Uncertainty in Repeated Measurements of data processing by [42].

From obtained measurement, after excluding a pressure drops on hydraulic tee fitting and hose connections, the actual fluid pressure on inlet and outlet of high-pressure hoses and high-pressure hose with repairing fitting is presented in Fig. 5.

Four measurements, for each high-pressure hose type, to eliminate data distortion (error between measurements) have been provided and is shown in Table 2.

Table 2. Percentage error between measurements

Nº of fluid pressure measurement	Error value at high-pressure hose, %	Error value at at high-pressure hose with repairing fitting, %
1 st measurement	1.04	1.28
2 nd measurement	0.98	1.19
3 rd measurement	1.14	1.31
4 th measurement	1.09	1.07

The nominal fluid pressure different between inlet and outlet of high-pressure hoses is $\sim 0.108 \cdot 10^6$ Pa for non-repaired high-pressure hose; $\sim 0.151 \cdot 10^6$ Pa for repaired hoses was obtained. According to measuring and by graph can be pointed the installation of repair fitting inside high-pressure hose lead to incise the pressure losses inside a hydraulic drive system.

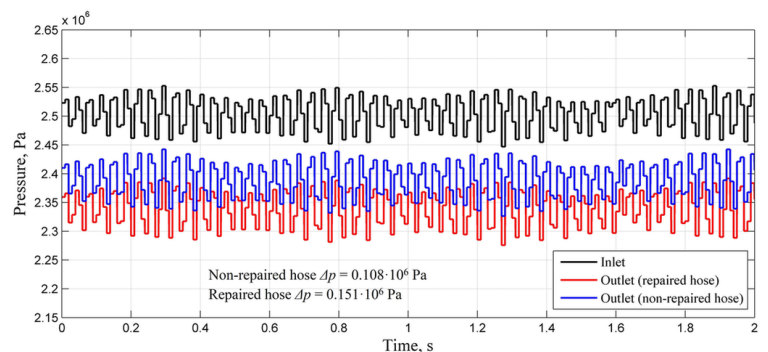


Fig. 5. The fluid pressure inside high-pressure hoses

5. Numerical modelling of fluid flow inside high-pressure hoses

Fluid movement is considered in 3D. Velocity (u, v, w) with a pressure depends on coordinates (x, y, z) and time (t). The dynamics of the fluid flow is governed by Navier–Stokes equations and is represented by the conservation of momentum. Thus, from mass conservation, the divergence of the velocity field is equal to zero ($\nabla u = 0$) [36, 41]. Movement and continuity equations for a viscous, compressible fluid in the research high-pressure hoses have the following form [12, 40]:

$$\begin{cases} \frac{\partial(\rho u)}{\partial t} + \frac{\partial(\rho u^2)}{\partial x} + \frac{\partial(\rho uv)}{\partial y} + \frac{\partial(\rho uw)}{\partial z} = -\frac{\partial p}{\partial x} + \frac{1}{\text{Re}} \left[\frac{\partial \tau_{xx}}{\partial x} + \frac{\partial \tau_{xy}}{\partial y} + \frac{\partial \tau_{xz}}{\partial z} \right], \\ \frac{\partial(\rho v)}{\partial t} + \frac{\partial(\rho uv)}{\partial x} + \frac{\partial(\rho v^2)}{\partial y} + \frac{\partial(\rho vw)}{\partial z} = -\frac{\partial p}{\partial y} + \frac{1}{\text{Re}} \left[\frac{\partial \tau_{xy}}{\partial x} + \frac{\partial \tau_{yy}}{\partial y} + \frac{\partial \tau_{yz}}{\partial z} \right], \\ \frac{\partial(\rho w)}{\partial t} + \frac{\partial(\rho uw)}{\partial x} + \frac{\partial(\rho vw)}{\partial y} + \frac{\partial(\rho w^2)}{\partial z} = -\frac{\partial p}{\partial z} + \frac{1}{\text{Re}} \left[\frac{\partial \tau_{xz}}{\partial x} + \frac{\partial \tau_{yz}}{\partial y} + \frac{\partial \tau_{zz}}{\partial z} \right], \end{cases} \quad (1)$$

$$\frac{\partial \rho}{\partial t} + \frac{\partial(\rho u)}{\partial x} + \frac{\partial(\rho v)}{\partial y} + \frac{\partial(\rho w)}{\partial z} = 0. \quad (2)$$

Computations of fluid flow inside high-pressure hoses were carried out employing commercial CFD software Ansys® Fluent®. The Standard $k-\varepsilon$ turbulence model was selected to analyse fluid flow. For the application of the Standard $k-\varepsilon$ turbulence model, the following transport equations for turbulent kinetic energy (k) and turbulent dissipation (ε) are implemented by [18, 21]:

$$\frac{\partial}{\partial t}(\rho k) + \frac{\partial}{\partial x_i}(\rho k u_i) = \frac{\partial}{\partial x_j} \left[\left(\mu + \frac{\mu_t}{\sigma_k} \right) \frac{\partial k}{\partial x_j} \right] + 2\mu_t E_{ij} E_{ij} - \rho \varepsilon, \quad (3)$$

$$\frac{\partial}{\partial t}(\rho \varepsilon) + \frac{\partial}{\partial x_i}(\rho \varepsilon u_i) = \frac{\partial}{\partial x_j} \left[\left(\mu + \frac{\mu_t}{\sigma_\varepsilon} \right) \frac{\partial \varepsilon}{\partial x_j} \right] + C_{1\varepsilon} \frac{\varepsilon}{k} (2\mu_t E_{ij} E_{ij}) - C_{2\varepsilon} \rho \frac{\varepsilon^2}{k}.$$

$$\mu_t = \rho C_\mu k^2 / \varepsilon. \quad (4)$$

$C_{1\varepsilon}, C_{2\varepsilon}, C_\mu, \sigma_k, \sigma_\varepsilon$ – constants for Standard $k-\varepsilon$ turbulence model (Table 3).

Multiphase simulation involves homogenous material, i.e. stand-
Table 3. Constants for Standard $k-\varepsilon$ turbulence model

$C_{1\varepsilon}$	$C_{2\varepsilon}$	C_μ	σ_k	σ_ε
1.44	1.92	0.09	1.00	1.30

ard mineral hydraulic oil Hydraux HLP 46, that conforms to the DIN 51524-2:2016 [14]. The specification of oil, used in simulations, are shown in Table 4.

Table 4. Oil (HLP 46) specification used in numerical simulation

Properties	Value
Molar mass	300 kg/kmol
Density	874 kg/m ³
Kinematic viscosity	46 mm ² /s
Specific heat capacity	1966 J/kg·K
Ref temperature	40 C°
Reference pressure	1·10 ⁵ N/mm ²
Thermal conductivity	0.292 W/m·K

In the Fig. 6 shows the applied boundary conditions used to solve the compressible Navier–Stokes equations with a Standard $k-\varepsilon$ turbulence model for fluid flow simulation inside high-pressure hoses.

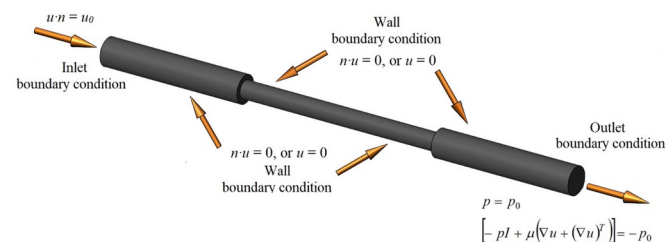


Fig. 6. Boundary conditions of the fluid flow for Ansys® Fluent® simulation

The inlet boundary and specified by a velocity vector what is normal to the inlet:

$$u \cdot n = u_0. \quad (5)$$

In the figure above and equation n is a unit vector that has a direction perpendicular to a boundary or normal to a boundary. For the outlet, certain pressure in the outlet/pressure boundary condition is imposed:

$$\begin{cases} p = p_0 \\ [-pI + \mu(\nabla u + (\nabla u)^T)] = -p_0. \end{cases} \quad (6)$$

The wall boundary condition states that due to fluid flow, the velocity of fluid near the wall is equal to zero:

$$n \cdot u = 0. \quad (7)$$

The numerical simulation of fluid flow inside high-pressure hoses was developed employing the Ansys® Workbench®. The numerical code was based on the Finite Volumes Method. The investigation area covered a 3D volume closed from all sides and divided into tetrahedrons. The dependent pressure, velocity and turbulent kinetic energy variables as well as volume fraction were calculated for each node of flow-element according to [2]. The mesh refined near changes in the cross-section area and around restrictive objects, according to [23], in order to obtain more accurate to experimental measurements. Close to the walls, boundary layers maximally affect velocity gradients in the normal direction to the wall. Thus, ten inflation layers were created with an expansion factor of 1.2...1.6 depending on changes in diameter. The mesh independence study was performed according to [19].

Ansys® Fluent® simulation was performed to established pressure drop (Δp) in research objects fluid flow and taken at a rate from 5 to 100 l/min. The Re number for both case is provided in the chart of Fig. 7. The total pressure profile of fluid inside repaired and non-repaired hoses are displayed in Fig. 8. The additional results of numerical simulation are provided in Fig. 9.

According to Reynolds number chart, the turbulence of fluid flow inside repaired hose started at the flow rate (in the inlet of hose) of

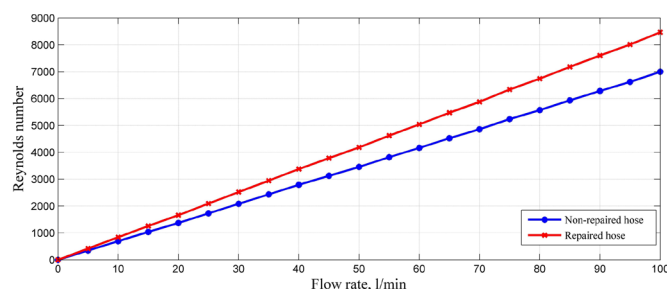


Fig. 7. The diagram of depending Re number from flow rate

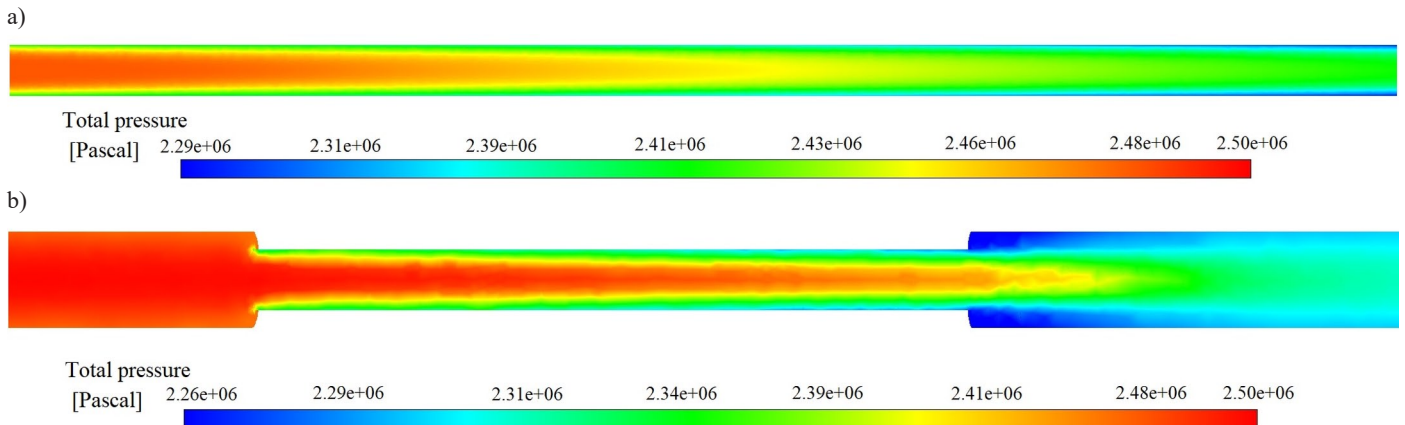


Fig. 8. Total fluid pressure inside high-pressure hoses: a) non-repaired hoses; b) repaired hose

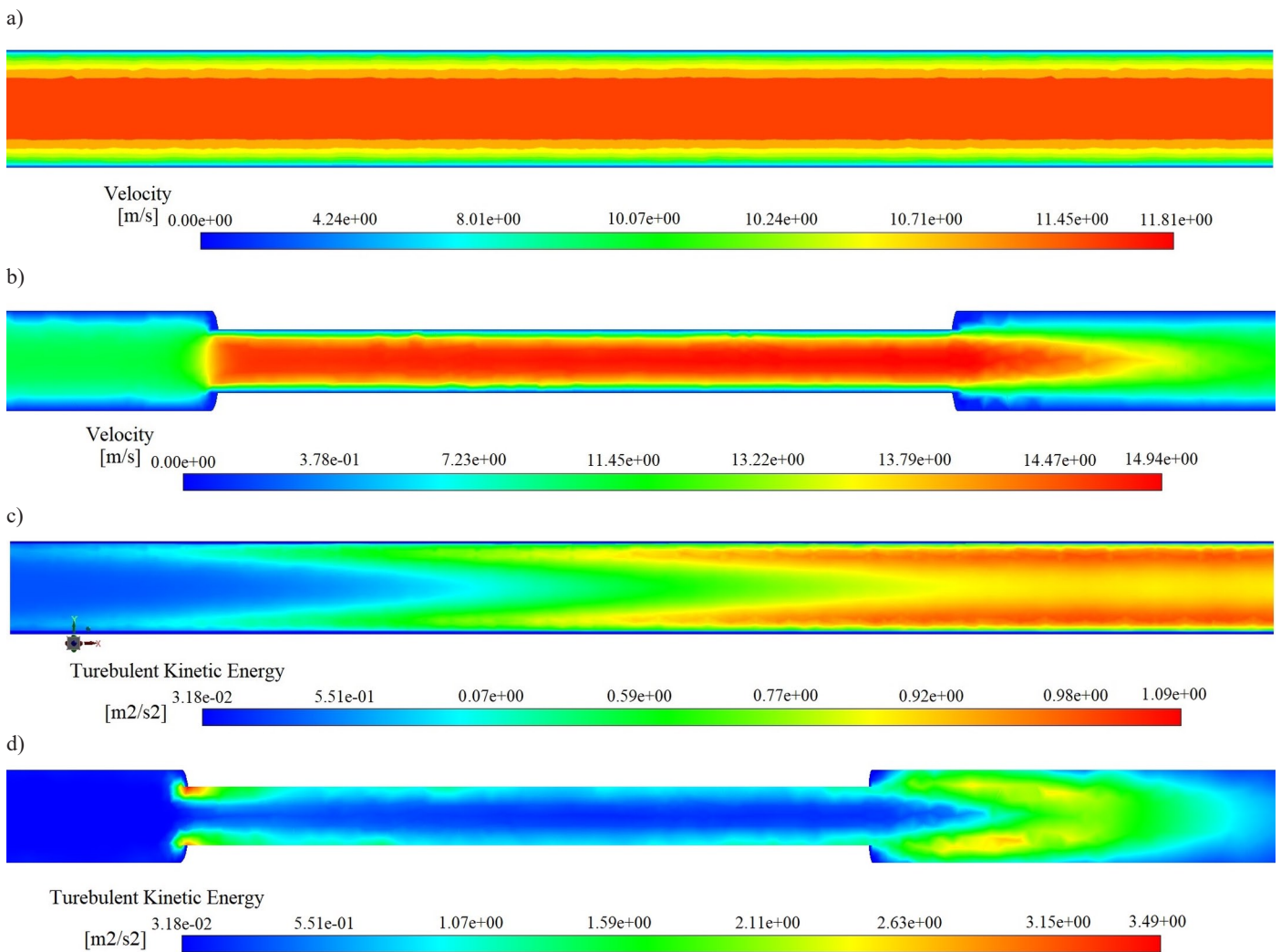


Fig. 9. Additional results from the fluent simulation: a) velocity inside non-repaired hose; b) velocity inside repaired hose; c) turbulence kinetic energy inside non-repaired hose; d) turbulence kinetic energy inside repaired hose

approximately 28 l/min, and that for non-repaired hose – at a flow rate of 34 l/min, which confirms that the installation of repairing fitting, during maintenance, significantly influenced on fluid flow inside a high-pressure hoses.

All above introduced results were taken from Ansys® Fluent® simulation where in inlet upload velocity was 11.764 m/s, which corresponded to the flow rate of 50 l/min in the inlet of hoses.

The flow coefficient (μ) is a relative measure of high-pressure hose efficiency at an allowed fluid flow. The coefficient describes the re-

lationship between pressure drop (Δp) across the orifice and the corresponding flow rate:

$$\mu = \frac{Q}{A \sqrt{\frac{1}{1-b^4} \sqrt{2\Delta p / \rho}}} \quad (8)$$

where $b = d/D$, where b – cross section diameter of fluid flow, m; D – diameter of the high-pressure hose, m; d – diameter of repair-

ing fitting, m; Q – flow rate, m³/s; A – average cross-section area of hose before and after repairing, m²; Δp – pressure drop, Pa; ρ – fluid density, kg/m³.

For repaired and non-repaired high-pressure hoses the funded flows coefficient is shown in Fig. 10.

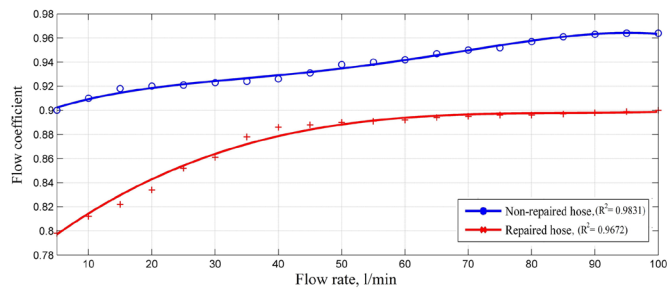


Fig. 10. Flow coefficient at a different flow rate for repaired and non-repaired hoses

The research demonstrated that non-repaired hose performed in the most efficient way (flow coefficient ranged from 0.91 to 0.962) than repaired hose (from 0.798 to 0.903). The difference between changes in the cross-section areas had a significant impact on flow characteristics. Changes in the cross-section areas of repaired hose were higher than those in standard hose. Difference between flow coefficients, which made ~ 14% at the beginning of the chart (laminar processes) is observed. However, in terms of the turbulence of flow processes, the two type of hoses have the more close flow characteristics. The difference in the flow coefficient, because of flow turbulence, between repaired and non-repaired hoses was ~ 9%. This proves that changes in the cross-section areas inside investigated hoses had more influence on laminar flow's processes than on flow's turbulence.

According to proposed numerical model of the determination hydrodynamic processes inside repaired and non-repaired high-pressure hoses the pressure losses, as well as flow coefficients can be established. The obtained results will help for evaluation the power losses on different flow rate inside investigated hoses.

6. Analysis of the energy efficiency

According to [7] and [24] researches – the less pressure drops exist in a system, the less power cost of hydraulic units can be obtained. According to achieved results of pressure losses from numerical modelling, power losses at each type of hoses were calculated by different flow rates. Power losses (N_l) are calculated using equation:

$$N_l = \frac{1}{\eta_p \eta_d} Q_i \Delta p_i, \quad (9)$$

where Δp_i – hydraulic losses at the i -th hydraulic hose of the system; η_p – overall efficiency of hydraulic pump; η_d – efficiency of the pump-motor drive; Q_i – flow rate at the i -th hydraulic hose of the system.

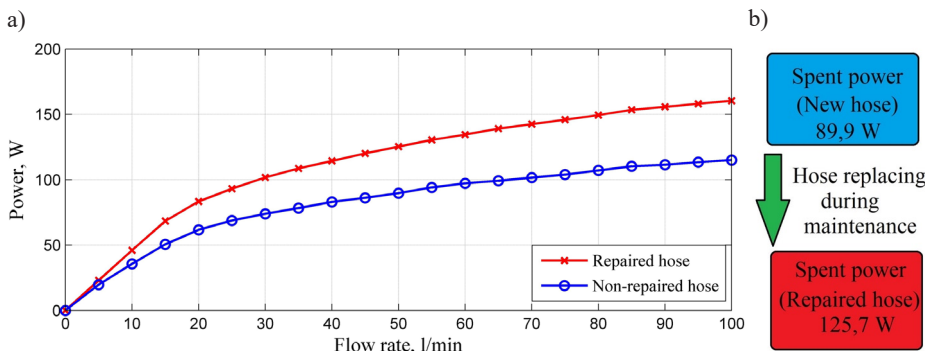


Fig. 11. Energy graphs: a) graph of power losses using repaired and non-repaired high-pressure hoses; b) the energy flow chart when high-pressure hose during maintenance is repaired

Power losses by using repaired and non-repaired hoses for hydraulic drive is presented in Fig. 11a (by one meter of each high-pressure hose).

Research on power losses in repaired hoses demonstrate insignificant power losses (from 22.98 W to 160.34 W at flow rate from 5 l/min to 100 l/min) compared to non-repaired hose (ranged from 7.85 W to 131.42 W). Although the pressure losses for one repaired hoses are not significant, but in modern transport vehicles hydraulic drive can be over than 100 high-pressure hoses. Even if 10% from all hoses of the system will be repaired that significantly effects on the resistance and loss in all hydraulic system.

The analysis of the investigated high-pressure hoses energy efficiency and its influence on the hydraulic system is presented on example by applied parameters of hydraulic system by experimental measuring and validated fluent model, by flow rate – 50 l/min (middle range). The energy flow charts (Fig. 11b) is applicable for illustration energy transformation visually and quantitatively during replacing damaged high-pressure hose by repaired hose with junction fitting. The obtained results showed that the better options for energy saving in the hydraulic drive could be reached using non-repaired hose (spent power – 89.9 W), compared to repaired hose (spent power – 125.7 W), on length one meter. The difference on spent power 35.8 W (28.4%) compared to whole hydraulic power is a not significant, but taking in an account the sum of all repaired hoses in the system and time of machinery operation during the year, from the economical side the changes of damages hoses on a new can be more rational than repairing hose during a maintenance. For future research, it will be useful to investigate the compact versions of high-pressure hoses after repairing with expand experimental setup and numerical simulation taking in account a temperature analysis and hoses vibration, since installation of repairing fitting influence on hose mechanical behaviour.

7. Conclusion

In the present research, by experimental measuring's and numerical simulation, compared a repaired high-pressure hose and non-repaired hose. As a result of the research, pressure drops at different fluid flow rates (from 5 to 100 l/min), hence flow coefficients was determined. Was found that non-repaired hose performed in the most efficient way (flow coefficient ranged from 0.91 to 0.962) than repaired hose (flow coefficient ranged from 0.798 to 0.903).

The difference between changes in the cross-section areas had a significant impact on flow characteristics. Changes in the cross-section areas of repaired hose were higher than those in non-repaired hose. Difference between flow coefficients, which made around 14% at the laminar processes and around 9% at turbulent processes is observed. The results was identified that turbulence started in repaired hoses at a range of 28 l/min, which explained a significant jump in the flow coefficient. As for the non-repaired hose turbulent processes started following 34 l/min, because changes in the hydraulic diameter hardly occurred in the case of the straight pipeline.

By the proposed numerical model of the determination hydrodynamic processes inside repaired and non-repaired high-pressure hoses the pressure losses was established, what held to evaluate the power losses on different flow rate inside investigated hoses. Research on power losses in repaired hoses demonstrated insignificant power losses from 22.98 W to 160.34 W, compared to non-repaired hose, ranged from 7.85 W to 131.42 W.

In final it was disclosed that repairing of the hose with a junction fitting lead to achieve an increase of power losses and decrease hydraulic drive efficiency by replac-

References

1. ANSYS Fluent Theory Guide, 2013. ANSYS, Inc., 275 Technology Drive Canonsburg, PA 15317.
2. Biluš I, Škerget L, Predin A, Hriberšek M. Experimental and numerical analyses of the cavitation flows around a hydrofoil. *Strojniški vestnik - Journal of Mechanical Engineering* 2005; 51(2): 103-118.
3. Bogdevičius P, Prentkovskis O, Bogdevičius M. Transmission with cardan joint parametre influence to centrifugal pump characteristics. *Mokslas – Lietuvos Ateitis / Science – Future of Lithuania* 2017; 9(5): 559-564, <https://doi.org/10.3846/mla.2017.1073>.
4. Budinski M. Failure analysis of a rubber hose in anhydrous ammonia service. *Case Studies in Engineering Failure Analysis* 2013; 1(2): 156-164, <https://doi.org/10.1016/j.csefa.2013.04.009>.
5. Cho J. Anisotropic large deformation and fatigue damage of rubber-fabric braid layered composite hose. *Procedia Engineering* 2017; 173: 1169-1176. <https://doi.org/10.1016/j.proeng.2016.12.097>.
6. Doerfler P, Sick M, Coutu A. Flow-induced pulsation and vibration in hydroelectric machinery. *Engineer's guidebook for planning design and troubleshooting*, Springer-Verlag 2013: 242, <https://doi.org/10.1007/978-1-4471-4252-2>.
7. Domagała Z, Kędzia K, Stosiak M. The use of innovative solutions improving selected energy or environmental indices of hydrostatic drives. *IOP Conference Series. Materials Science and Engineering* 2019; 679(1): 12, <https://doi.org/10.1088/1757-899X/679/1/012016>.
8. Drumond G, Pasqualino I, Ferreira da Costa M. Study of an alternative material to manufacture layered hydraulic hoses. *Polymer Testing* 2016; 53: 29-39, <https://doi.org/10.1016/j.polymertesting.2016.05.003>.
9. European standard. EN 853 2SN:2015. Rubber hoses and hose assemblies. Wire braid reinforced hydraulic type. Specification 2015; 17.
10. Fedorko G, Molnar V, Dovicab M, Toth T, Fabianova J. Failure analysis of irreversible changes in the construction of the damaged rubber hoses. *Engineering Failure Analysis* 2015; 58(1): 31–43, <https://doi.org/10.1016/j.engfailanal.2015.08.042>.
11. Firoozabad E, Jeon B, Choi H, Kim N. Failure criterion for steel pipe elbows under cyclic loading. *Engineering Failure Analysis* 2016; 66: 515-525, <https://doi.org/10.1016/j.engfailanal.2016.05.012>.
12. Foias C, Manley O, Rosa R, Temam R. Navier-Stokes equations and turbulence (Encyclopedia of Mathematics and its Applications). Cambridge: Cambridge University Press 2001; 347, <https://doi.org/10.1017/CBO9780511546754>.
13. Gates Corporation. A Guide to Preventive Maintenance & Safety for Hydraulic Hose & Couplings. Printed in Denver, USA by Tomkins Company 2009; 76, <http://www.marshall-equipment.com/Library/SafeHydraulics.pdf>.
14. German Institute for Standardisation. DIN 51524-2:2016. Pressure Fluids – Hydraulic Oils – Part 2: HLP Hydraulic Oils, Minimum Requirements. Specification 2016; 11.
15. International Organization for Standardization. ISO 8434-1:2018. Metallic tube connections for fluid power and general use — Part 1: 24° cone connectors. Specification 2018; 51.
16. Karpenko M, Bogdevičius M. Review of energy-saving technologies in modern hydraulic drives. *Science – Future of Lithuania - Mokslas – Lietuvos Ateitis* 2017; 9(5): 553–558, <https://doi.org/10.3846/mla.2017.1074>.
17. Karpenko M, Bogdevičius M. Investigation of hydrodynamic processes in the system – “Pipeline-Fittings”. *TRANSBALTICA XI: Transportation Science and Technology. TRANSBALTICA 2020*; 331-340. *Lecture Notes in Intelligent Transportation and Infrastructure*. Springer, Cham, https://doi.org/10.1007/978-3-030-38666-5_35.
18. Karpenko M, Bogdevičius M. Investigation into the hydrodynamic processes of fitting connections for determining pressure losses of transport hydraulic drive. *Transport* 2020; 35(1): 108-120, <https://doi.org/10.3846/transport.2020.12335>.
19. Kubrak M, Malesińska A, Kodura A, Urbanowicz K, Stosiak M. Hydraulic transients in viscoelastic pipeline system with sudden cross-section changes. *Energies* 2021; 14(14): 4071, <https://doi.org/10.3390/en14144071>.
20. Kwak S, Choi N. Micro-damage formation of a rubber hose assembly for automotive hydraulic brakes under a durability test. *Engineering Failure Analysis* 2009; 16: 1262-1269, <https://doi.org/10.1016/j.engfailanal.2008.08.009>.
21. Launder B, Spalding D. Lectures in mathematical models of turbulence. Academic Press, London, England 1972; 16, <https://doi.org/10.1002/zamm.19730530619>.
22. Lee G, Kim H, Park J, Jin H, Lee Y, Kim J. An experimental study and finite element analysis for finding leakage path in high pressure hose assembly. *International Journal of Precision Engineering and Manufacturing* 2011; 12: 537–542, <https://doi.org/10.1007/s12541-011-0067-y>.
23. Lisowski E, Panek M. CFD modeling method of vanes working in the vane pump. *Eksplatacja i Niezawodność - Maintenance and Reliability* 2004; 2: 36-41.
24. Liu H, Zhang X, Quan L, Zhang H. Research on energy consumption of injection molding machine driven by five different types of electrohydraulic power units. *Journal of Cleaner Production* 2020; 242: 1–11, <https://doi.org/10.1016/j.jclepro.2019.118355>.
25. Lu X, Huang M. Novel multi-level modeling method for complex forging processes on hydraulic press machines. *The International Journal of Advanced Manufacturing Technology* 2015; 79: 1869–1880, <https://doi.org/10.1007/s00170-015-6970-0>.
26. Lubecki M, Stosiak M, Bocian M, Urbanowicz K. Analysis of selected dynamic properties of the composite hydraulic microhose. *Engineering Failure Analysis* 2021; 125: 1-9, <https://doi.org/10.1016/j.engfailanal.2021.105431>.
27. Luczko, J., Czerwiński, A. 2014. Parametric vibrations of pipes induced by pulsating flows in hydraulic systems, *Journal of Theoretical and Applied Mechanics*, 52 (3): 719–730.
28. Mazurkiewicz L, Malachowski J, Damaziak K, Tomaszewski, M. Evaluation of the response of fibre reinforced composite repair of steel pipeline subjected to puncture from excavator tooth. *Composite Structures* 2018; 202: 1126–1135, <https://doi.org/10.1016/j.compstruct.2018.05.065>.
29. Mikota G. Modal analysis of hydraulic pipelines. *Journal of Sound and Vibration* 2013; 332(16): 3794 – 3805, <https://doi.org/10.1016/j.jsv.2013.02.021>.
30. Miller S. Systematic techniques of hose failure mode analysis. *SAE Transactions* 1991; 100: 687–703, <http://www.jstor.org/stable/44632066>.
31. O'Brien P, Meldrum E, Overton C, Picksley J, Anderson K, Ian M. Outcomes from the SureFlex joint industry project - an international

- initiative on flexible pipe integrity assurance. Paper presented at the Offshore Technology Conference, Houston, Texas, USA, May 2011, <https://doi.org/10.4043/21524-MS>.
32. Parvaresh A, Mardani M. Model predictive control of a hydraulic actuator in torque applying system of a mechanically closed-loop test rig for the helicopter gearbox. *Aviation* 2019; 23(4): 143-153, <https://doi.org/10.3846/aviation.2019.11869>.
 33. Pavloušková Z, Klakurková L, Man O, Čelko L, Švejar J. Assessment of the cause of cracking of hydraulic hose clamps. *Engineering Failure Analysis* 2015; 56: 14-19, <https://doi.org/10.1016/j.engfailanal.2015.05.014>.
 34. Pelevin L, Machyshyn G, Bogdevičius M, Karpenko M. Assessment of application high pressure hoses using mathematical model calculation load distribution between the metal braid. *Mining, constructional, road and melioration machines: AllUkrainian collection of scientific works* 2016; 88: 64-70.
 35. Pierce S, Evans J. Failure analysis of a metal bellows flexible hose subjected to multiple pressure cycles. *Engineering Failure Analysis* 2012; 22: 11-20, <https://doi.org/10.1016/j.engfailanal.2011.12.005>.
 36. Santos F, Brito A, de Castro A, Almeida M, da Cunha Lima A, Zebende G, da Cunha Lima I. Detection of the persistency of the blockages symmetry on the multi-scale cross-correlations of the velocity fields in internal turbulent flows in pipelines. *Physica A: Statistical Mechanics and its Applications* 2018; 509(1): 294–301, <https://doi.org/10.1016/j.physa.2018.06.009>.
 37. Romaniuk M. Optimization of maintenance costs of a pipeline for a V-shaped hazard rate of malfunction intensities. *Eksploatacja i Niezawodność – Maintenance and Reliability* 2018; 20 (1): 46–56, <https://doi.org/10.17531/ein.2018.1.7>.
 38. Tawancy H, Al-Hadhrami L. Failure analysis of a welded outlet manifold pipe in a primary steam reformer by improper selection of materials. *Engineering Failure Analysis* 2009; 16(3): 816-824, <https://doi.org/10.1016/j.engfailanal.2008.07.001>.
 39. Taylor C, Thompson J, Handewith H, Thimons E. Hose safety during high-pressure water-jet cutting. *Information Circular by USA Bureau of Mines Information, Pittsburgh* 1987; 9.
 40. Urbanowicz K, Stosiak M, Towarnicki K, Bergant A. Theoretical and experimental investigations of transient flow in oil-hydraulic small-diameter pipe system. *Engineering Failure Analysis* 2021; 128: 105607, <https://doi.org/10.1016/j.engfailanal.2021.105607>.
 41. Urbanowicz K, Bergant A, Kodura A, Kubrak M, Malesińska A, Bury P, Stosiak M. Modeling transient pipe flow in plastic pipes with modified discrete bubble cavitation model. *Energies* 2021; 14(20):6756, <https://doi.org/10.3390/en14206756>.
 42. Vardeman S, Jobe M. *Statistical methods for quality assurance: basics, measurement, control, capability and improvement*. Part of the Springer Texts in Statistics book series (STS) Springer–Verlag, New York 2016: 437, <https://doi.org/10.1007/978-0-387-79106-7>.
 43. Wei Q, Huailiang Z, Wenqian S, Wei L. Stress response of the hydraulic composite pipe subjected to random vibration. *Composite Structures* 2021; 255: 1-8, <https://doi.org/10.1016/j.compstruct.2020.112958>.
 44. Yangyang Y, Mengjiang C. Sealing failure and fretting fatigue behavior of fittings induced by pipeline vibration. *International Journal of Fatigue* 2020; 136: 105602, <https://doi.org/10.1016/j.ijfatigue.2020.105602>.